Since January 2020 Elsevier has created a COVID-19 resource centre with free information in English and Mandarin on the novel coronavirus COVID-19. The COVID-19 resource centre is hosted on Elsevier Connect, the company's public news and information website.

Biosensors and Bioelectronics 25 (2009) 320–325

Contents lists available at ScienceDirect

Biosensors and Bioelectronics

journal homepage: www.elsevier.com/locate/bios

Detection of severe acute respiratory syndrome (SARS) coronavirus nucleocapsid protein in human serum using a localized surface plasmon coupled fluorescence fiber-optic biosensor

Jason C. Huang[a,c,e,1], Ying-Feng Chang[b,1], Kuan-Hsuan Chen[c,f,1], Li-Chen Su[d], Chun-Wei Lee[a,f], Chii-Chang Chen[d], Yi-Ming Arthur Chen[c,f,*], Chien Chou[b,d,g,**]

[a] Department of Biotechnology and Laboratory Science in Medicine, National Yang-Ming University, Taipei 112, Taiwan
[b] Institute of Biophotonics, National Yang-Ming University, Taipei 112, Taiwan
[c] AIDS Prevention and Research Center, National Yang-Ming University, Taipei 112, Taiwan
[d] Department of Optics and Photonics, National Central University, Taoyuan 320, Taiwan
[e] Department of Education and Research, Taipei City Hospital, Taipei 112, Taiwan
[f] Institute of Microbiology and Immunology, National Yang-Ming University, Taipei 112, Taiwan
[g] Graduate Institute of Electro-Optical Engineering, Chang Gung University, Taoyuan 333, Taiwan

ARTICLE INFO

Article history:
Received 1 June 2009
Received in revised form 8 July 2009
Accepted 10 July 2009
Available online 17 July 2009

Keywords:
Fiber-optic biosensor
Gold nanoparticle
Localized surface plasmon
Nucleocapsid protein
Severe acute respiratory syndrome (SARS)

ABSTRACT

In order to enhance the sensitivity of conventional immunoassay technology for the detection of SARS coronavirus (SARS-CoV) nucleocapsid protein (N protein), we developed a localized surface plasmon coupled fluorescence (LSPCF) fiber-optic biosensor that combines sandwich immunoassay with the LSP technique. Experimentally, a linear relationship between the fluorescence signal and the concentration of recombinant SARS-CoV N (GST-N) protein in buffer solution could be observed from 0.1 pg/mL to 1 ng/mL. In addition, the concentration of GST-N protein in diluted serum across a similar range could also be measured. The correlation coefficients (linear scale) for these two measurements were 0.9469 and 0.9624, respectively. In comparison with conventional enzyme linked immunosorbent assay (ELISA), the detection limit of the LSPCF fiber-optic biosensor for the GST-N protein was improved at least 10^4-fold using the same monoclonal antibodies. Therefore, the LSPCF fiber-optic biosensor shows an ability to detect very low concentration (~1 pg/mL) of SARS-CoV N protein in serum. The biosensor should help with the early diagnosis of SARS infection.

1. Introduction

Severe acute respiratory syndrome (SARS) is a highly infectious disease that results in death in a great portion of patients (Drosten et al., 2004). SARS is caused by the SARS coronavirus (SARS-CoV) which is detectable in respiratory secretions of patients after infection (Fouchier et al., 2003). This disease is highly contagious and still has the potential to cause a very large-scale epidemic in the future in the absence of a vaccine or effective therapeutic drugs (Wang et al., 2004). The key to preventing and controlling a future outbreak of SARS is to block transmissions of infection through a strict quarantine policy. Therefore, a rapid, sensitive, specific, and accurate diagnostic method is essential so that suspected patients can be correctly assessed (Jiang et al., 2004; Che et al., 2004). Currently, there are several diagnostic methods used for the detection of SARS. The first option is based on nucleic acid detection. Since the genome of SARS-CoV has been sequenced completely (Marra et al., 2003; Rota et al., 2003), reverse transcription-polymerase chain reaction (RT-PCR) is the most common method that is used to detect the SARS-CoV during the early phase immediately after the onset of clinical symptoms (Hourfar et al., 2004; Louie et al., 2006; Petrich et al., 2006). However, the RT-PCR assay is probably not sensitive enough to detect SARS-CoV in secretions or serum until 3 days after the onset of symptoms (Yam et al., 2003). Statistically, about half of SARS patients cannot be identified at an early stage based on viral RNA detection (Li et al., 2005). Besides, the RT-PCR tests require not only a thermal cycler for conventional PCR or a more complicated machine for real-time PCR (Liu et al., 2005), but also a specific laboratory with expertise in molecular diagnostics to confirm SARS in the acute phase (Drosten et al., 2004; Che et al., 2004; Fujimoto et al., 2008). Unfortunately, other sequence based methods such

* Corresponding author at: AIDS Prevention and Research Center, National Yang-Ming University, Taipei 112, Taiwan. Tel.: +886 2 28267193; fax: +886 2 28270576.
** Corresponding author at: Graduate Institute of Electro-Optical Engineering, Chang Gung University, Taoyuan 333, Taiwan. Tel.: +886 3 2118800x3677; fax: +886 3 2118507.
E-mail addresses: arthur@ym.edu.tw (Y.-M.A. Chen), cchou@mail.cgu.edu.tw (C. Chou).
[1] Equal contribution in this research.

0956-5663/$ – see front matter © 2009 Elsevier B.V. All rights reserved.
doi:10.1016/j.bios.2009.07.012

as a real-time loop-mediated amplification assay (Poon et al., 2004, 2005; Hong et al., 2004), a gold film with enzymatic electrochemical genosensor (Abad-Valle et al., 2005) and a rolling circle amplification PCR-based assay (Wang et al., 2005) exhibit lower sensitivity than the RT-PCR method. Serological testing is another diagnostic option. However, serological tests have shown a relatively low sensitivity of only 65.4% using sera obtained 6–10 days after the onset of symptoms (Shi et al., 2004). The third option is based on detecting antibodies against SARS-CoV after infection (Peiris et al., 2003a). However, the antibody response in more than 93% of SARS patients takes at least 10–28 days to develop after symptoms onset, so this approach is not a good method for early detection (Peiris et al., 2003b). The final possible approach is to detect specific SARS-CoV antigens such as the spike protein (Zhao et al., 2005; Haynes et al., 2007; Manopo et al., 2005) and particularly the nucleocapsid (N) protein. The N protein is one of the early expressed proteins and should have diagnostic value. In the serum of SARS patients, it has been shown that N protein can be detected as early as 1 day after infection (Che et al., 2004). Thus, detection of SARS-CoV N proteins is a valuable approach to diagnose and monitor disease activity and makes it possible to develop a rapid and accurate diagnostic method at an early stage. In addition, one significant advantage of detecting SARS-CoV N protein in serum is to eliminate the risk of infection while collecting nasopharyngeal aspirates (Che et al., 2004). Among several possible methods are available for the detection of SARS-CoV N protein, conventional antigen capture enzyme-linked immunosorbent assay (ELISA) is the most widely used method (Chen et al., 2005; Chan et al., 2005; Qiu et al., 2005). Yet another method of detecting SARS-CoV N protein is based on an immunofluorescence assay, which was able to detect SARS-CoV from SARS patients as early as 2 days after the onset of symptoms (Liu et al., 2005). Recently, Professor Okamoto and his co-workers proposed a highly sensitive immunoassay based on an enzyme-linked immunosorbent assay using chemiluminescence (CLEIA) for the detection of SARS-CoV N protein and this method has pushed the detection limit to 1.56 pg/mL (Fujimoto et al., 2008).

Recently, gold nanoparticles (GNPs) have been introduced into biosensing and proved to be one of the most efficient ways to increase the detection limit of biosensors (Manso et al., 2008; Cui et al., 2008). It is well known that GNPs possess special optical properties such as localized surface plasmons (LSPs) which result in wavelength selective absorption with extremely large molar extinction coefficients and significant enhancement of the localized electromagnetic field close to the GNP surface within 50–60 nm (Mock et al., 2003; Sonnichsen et al., 2002; McFarland and Van Duyne, 2003). Based on the property of localized surface plasmon coupled fluorescence (LSPCF) combined with the sandwich immunoassay, a novel fiber-optic biosensor has been proposed by our group to study protein–protein interactions. Experimentally, the detection limit of LSPCF fiber-optic biosensor has been demonstrated to be as low as 1 pg/mL when detecting mouse immunoglobulin G (IgG) interacting with anti-mouse IgG (Hsieh et al., 2007). In addition, we have also demonstrated that the LSPCF fiber-optic biosensor is able to measure alpha-fetoprotein in human serum as low as 0.1 ng/mL (Chang et al., 2009). In this report, the LSPCF fiber-optic biosensor is applied to enhance the detection sensitivity of SARS-CoV N protein in diluted serum to a limit of 0.1 pg/mL. Clearly, the biosensor has significant potential for the early detection of clinical SARS-CoV infection.

2. Materials and methods

2.1. Materials

Human serum was prepared from a healthy donor. Bovine serum albumin (BSA); GNP conjugate protein A (Au-PA, GNP diameter = 20 nm); phosphate buffer saline (PBS) tablet; ethyl acetate and 2-propanol were purchased from Sigma Inc. (St. Louis, MO, USA). The fluorescent labeling kit (DyLight™ 649) was purchased from Pierce Co. (Rockford, IL, USA). The plastic optical fiber was purchased from Mitsubishi Rayon Co., LTD. (Tokyo, Japan).

2.2. Plasmid construction

The RNA genome sequence of SARS-CoV was utilized as a template to synthesize the cDNA sequence with the proper codon usage for *E. coli*. The cDNA sequence encoding the N protein was synthesized by RT-PCR reaction using the specific primers, F5′-GCCGAATTCATGTCTGATAA TGGACCCCA-3′ and R5′-GCGCGTCGACGTTATGCCTGAGTTGAATCA-3′. The cDNA fragment (1.3 kD) of N protein so obtained was digested with *Eco*RI and *Sal*I restriction enzymes and then ligated into the vector, pGEX-5X-1, which contains a glutathione S-transferase (GST) tag sequence. The expression vector encoding recombinant SARS-CoV N protein was named GST-N protein.

2.3. Expression and purification of recombinant SARS-CoV N protein

The GST-N plasmid was transformed into *E. coli* BL21 for expression of recombinant SARS-CoV N protein. After 3 h of induction with isopropyl-β-D-thiogalactopyranoside (IPTG) (1 mM), the bacteria were harvested and pellet resuspended in NETN buffer (20 mM Tris base in pH 8.0, 100 mM NaCl, 1 mM EDTA and 0.5% NP-40) for protein purification. The protein mixture was next incubated with glutathione-agarose beads (Sulphur linkage, Sigma St. Louis, MO, USA,) for 12 h. After the elution, the GST-tagged N protein was concentrated for immunization.

2.4. Preparation of anti-SARS-CoV N protein antibodies

Six-week-old BALB/c mice were immunized and twice-boosted with 25 μg of GST-N protein in 0.1 mL of PBS emulsified with an equal volume mixture of complete/incomplete Freund's adjuvant (Sigma, St. Louis, MO, USA). After the antibody titers against GST-N protein had been confirmed by ELISA and immunoblotting, splenocytes were harvested and fused with NS-1 myeloma cells. The hybridoma culture supernatants were then screened by ELISA and immunoblotting against the GST-N protein. Single clones producing a specific antibody were selected by the limiting dilution method. Polyclonal antibodies against GST-N protein were also prepared using New Zealand white rabbits, which were immunized and boosted with 100 μg of GST-N proteins in 0.5 mL PBS emulsified with an equal volume mixture of complete/incomplete Freund's adjuvant twice or three times. After the antibody titers against GST-N fusion protein were confirmed, then blood was taken from the rabbits for further purification. The monoclonal and polyclonal antibodies were purified from mouse ascites and rabbit serum, respectively, using protein A affinity columns (GE Healthcare, Buckinghamshire, UK). Two monoclonal antibodies against GST-N protein used in this study and were named anti-N-1 antibody and anti-N-2 antibody.

2.5. Immunoblotting analysis

In total, 1.0 μg of purified GST-N protein was loaded into each well of a 10% sodium dodecyl sulfate (SDS)-polyacrylamide gel for electrophoresis. After the transfer of the separated proteins to polyvinylidene difluoride membrane (PVDF) (Millipore, Billerica, MA, USA), the blot was cut into strips and incubated separately with 2.5 μg/mL of anti-N-1 antibody or 5 μg/mL of anti-N-2 antibody.

The blots were then washed and incubated with peroxidase-conjugated anti-mouse secondary antibody. Finally, the proteins on the strips were visualized using the Western Lightning Plus chemiluminescence reagent (PerkinElmer) and X-ray film exposure.

2.6. Conventional ELISA for GST-N protein detection

Immunoplates (PerkinElmer, Shelton, CT, USA) were first coated with 100 μL of 4.0 μg/mL anti-N-1 and anti-N-2 monoclonal antibodies (the capture antibody) at room temperature overnight. After blocking with 5% nonfat milk in PBST (PBS buffer containing 0.05% Tween 20) for 1 h, 100 μL of serially diluted GST-N proteins in PBS or 10-fold diluted human serum were added into each well and incubated at 37 °C for 2 h. The plates were then washed five times and 100 μL of anti-GST-N protein polyclonal antibody (5 μg/mL) was added with 2 h incubation at 37 °C. Correctly diluted peroxidase-conjugated anti-rabbit antibody was then added and incubated at 37 °C for 1 h after washing. Finally 75 μL of TMB/TBABH substrate solution per well was added and color developed for 10 min before termination with 125 μL of H_2SO_4 stop solution (1 M). The optical absorbance at 450 nm was measured by ELISA reader (Bio-Tek Inc. Winooski, VT, USA). A blank control in the absence of GST-N protein was included for normalization of the absorbance. Each dilution was performed in duplicate.

2.7. Preparation of optic fiber and setup of biosensor

A plastic (polymethyl methacrylate, PMMA) multimode optical fiber of 1 mm in diameter was used in this experiment. The PMMA fiber was de-clad by immersing the fiber in ethyl acetate. Subsequently, the declad portion of fiber was washed with 2-propanol to clean the declad surface. Chemical adsorption was carried out using covalent binding forces in order to immobilize the capture antibody onto the surface of declad portion. The protocol of chemical adsorption has been described previously (Chang et al., 2009). The modified declad portion of each optical fiber was first coated with 1 mL of 1 μg/mL anti-N-1 monoclonal antibody (capture antibody) at 4 °C overnight. The calculated surface concentration of immobilized capture antibody on PMMA fiber surface is $4.935\ \text{ng/mm}^2 < \Gamma < 5.758\ \text{ng/mm}^2$ approximately (Jung et al., 1998; Yu et al., 2004). After blocking with 10 mg/mL BSA-PBS solution for 1 h, 1 mL of serially diluted GST-N proteins in PBS and in 10-fold diluted human serum were added into each reaction chamber and incubated at 4 °C for 2 h in order to form the < capture antibody/target antigen> complex on the modified declad portion of fiber surface as shown in supplemental information Figure 1. Then, the fibers were washed five times.

2.8. Preparation of the fluorescence probe

The fluorescence probe is composed of fluorophores which are labeled with secondary antibodies connecting to Au-PA. The secondary antibody is anti-N-2 monoclonal antibody fluorescently labeled with DyLight™ 649 utilizing a commercial labeling kit. To produce the fluorescence probe, 100 ng/mL of fluorophore-labeled anti-N-2 antibody was mixed with Au-PA at a concentration of 9×10^9 particles/mL and incubated for 1 day at 4 °C in the dark.

2.9. Measurement

A 658 nm diode laser (Micro Laser System, Garden Grove, CA) was used as the excitation light source and a microscope objective (20×, NA = 0.45) was used in order to achieve the best coupling efficiency. The fluorophore, of which the central wavelength of the emission spectrum was 674 nm, was excited by the enhanced localized electromagnetic field close to the GNP surface during measurement. A narrow band pass filter (central wavelength = 680.4 nm; bandwidth = 11.1 nm) was introduced into this setup to allow fluorescence detection via a photomultiplier tube (PMT, R3896 Hamamatsu, Shizuoka, Japan). Experimentally, a lock-in amplifier (SR830, Stanford Research Systems, Sunnyvale, CA) was used in order to increase the signal to noise ratio (SNR). From the specifications of R3896 and SR830, the detection sensitivity of smallest detectable fluorescence signal is equal to 4.21×10^{-5} luminance.

3. Results

In order to generate monoclonal and polyclonal antibodies against SARS-CoV N protein, we created a recombinant N protein fused with GST that was expressed in *Escherichia coli*. The recombinant GST-N protein of 72 kD was detected by SDS-PAGE and is shown in supplemental information feature 2A. Hybridoma cells were prepared from mice immunized with GST-N protein and monoclonal antibodies were purified from culture supernatant of these hybridoma cells. The reactivity of the two monoclonal antibodies (anti-N-1 and anti-N-2) against the GST-N protein used in this study is presented in supplemental information feature 2B. The next step was to establish an antigen-capture system for SARS-CoV that would allow the concentration of GST-N protein to be determined by ELISA. Since the monoclonal antibodies were both derived from mouse, it is not possible to use them as the capture and detection

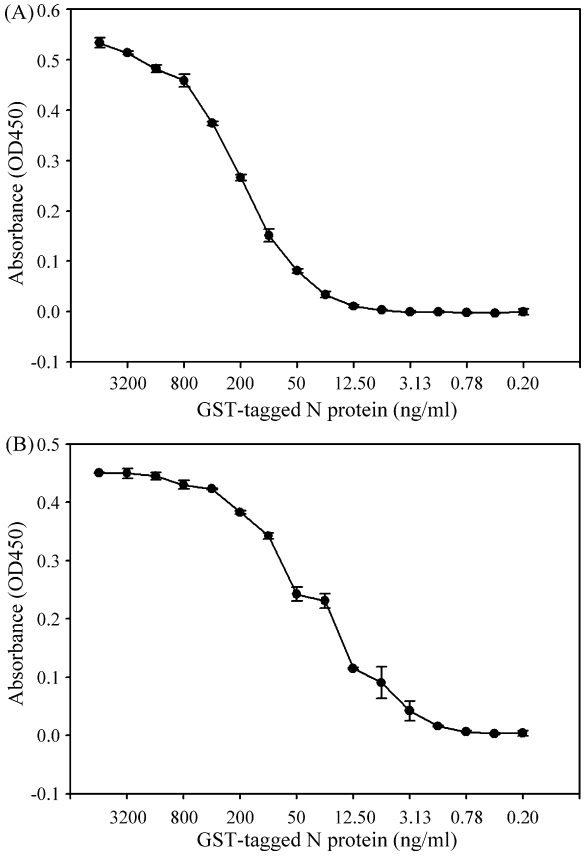

Fig. 1. Detection of GST-N protein by conventional sandwich ELISA. (A) Serially diluted GST-N proteins in PBS were detected by sandwich ELISA. Different concentrations of GST-N protein were assayed on a microtiter plate coated with anti-N-1 and anti-N-2 monoclonal antibodies. The absorbance of OD450 in each well was observed after further incubation with polyclonal anti-GST-N antibody followed by peroxidase-conjugated anti-rabbit antibody. (B) GST-N protein was serially diluted in 10-fold diluted human serum and assayed by ELISA. Results shown are the mean of duplicates. Error bars indicate the standard deviation.

antibodies because the secondary anti-mouse IgG will bind to both murine antibodies. Therefore, we immobilized both anti-N-1 and anti-N-2 antibodies on ELISA plates as the capture antibodies for the GST-N protein and used rabbit polyclonal anti-GST-N antibodies as the detection antibody. Various concentration of GST-N protein was diluted in PBS (6400–0.2 ng/mL) and the ELISA results are shown in Fig. 1A. In this sandwich ELISA, GST-N protein was successfully detected at concentrations as low as 12.5–25 ng/mL. In order to examine whether serum proteins might interfere with the antigen capture of SARS-CoV N protein, another ELISA was carried with various concentration of GST-N protein diluted using 10-fold diluted human serum. As shown in Fig. 1B, in this circumstance the GST-N protein can be detected down to the range of 0.78–1.56 ng/mL.

The temporal fluorescence intensity of biomolecular interaction between the LSPCF probe and GST-N protein in PBS at different concentrations is shown in Fig. 2A. The concentrations of GST-N protein at 0 pg/mL, 0.1 pg/mL, 1 pg/mL, 10 pg/mL, 100 pg/mL, and 1 ng/mL were tested separately. When a fixed concentration of LSPCF probes was injected into the reaction chamber, a great number of LSPCF probes migrated into the interaction region of the evanescent field near fiber core surface. Consequently, a rapid increase in fluorescence intensity at the beginning of the assay is observed. However, not all LSPCF probes in the interaction region bind to GST-N proteins (target antigens) which are captured by the immobilized anti-N-1 antibodies (capture antibodies) on the fiber core surface. In these circumstances, the LSPCF probes that are not associated with the antigens diffuse out of the interaction region of the evanescent field such that the fluorescence intensity decreases sharply. In addition, when LSPCF probes are injected into the reaction chamber, this induces the disturbance that results in decreasing of fluorescence signal in the measurement. Finally the signal reaches equilibrium as shown in Fig. 2A. The SNR in this experiment was better than 9 at different concentrations of GST-N protein in PBS if the PBS group is treated as a zero concentration solution (0 pg/mL of GST-N protein) to define background noise. The fluorescence signal is calculated by subtracting the background level from the detected fluorescence intensity in this experiment. The detected fluorescence intensity was obtained by averaging the signal over the last fifty data points for each concentration measurement. The standard deviation of the detected fluorescence intensity is equal to the noise level. The unit of fluorescence intensity is an arbitrary unit (a.u.) defined by the detected fluorescence intensity normalized against the intensity of the laser beam. In these conditions, it was possible to obtain a linear relationship between the fluorescence signal and GST-N protein concentration over the range from 0.1 pg/mL to 1 ng/mL as shown

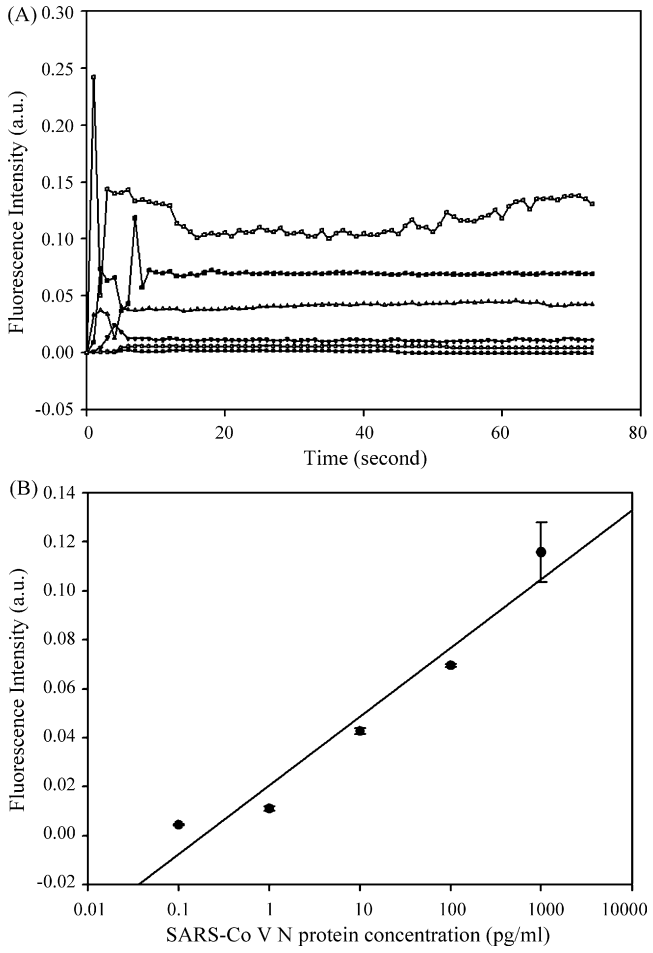

Fig. 2. Detection of different concentrations of GST-N protein in PBS with the LSPCF fiber-optic biosensor. (A) The binding processes of fluorescence probe interaction with different concentrations of GST-N protein in PBS [●: 0 pg/mL; ○: 0.1 pg/mL; ▼: 1 pg/mL; ▽: 10 pg/mL; ■: 100 pg/mL; □: 1000 pg/mL]. The uncertainty of the measurement is smaller than the size of data points in this figure. (B) The linear relationship [$y = 0.0122\,\mathrm{Ln}(x) + 0.0206$; $R^2 = 0.9469$] of GST-N protein concentration in PBS versus fluorescent signal. The error bar is smaller than the size of data points and equivalent to one standard derivation in this experiment.

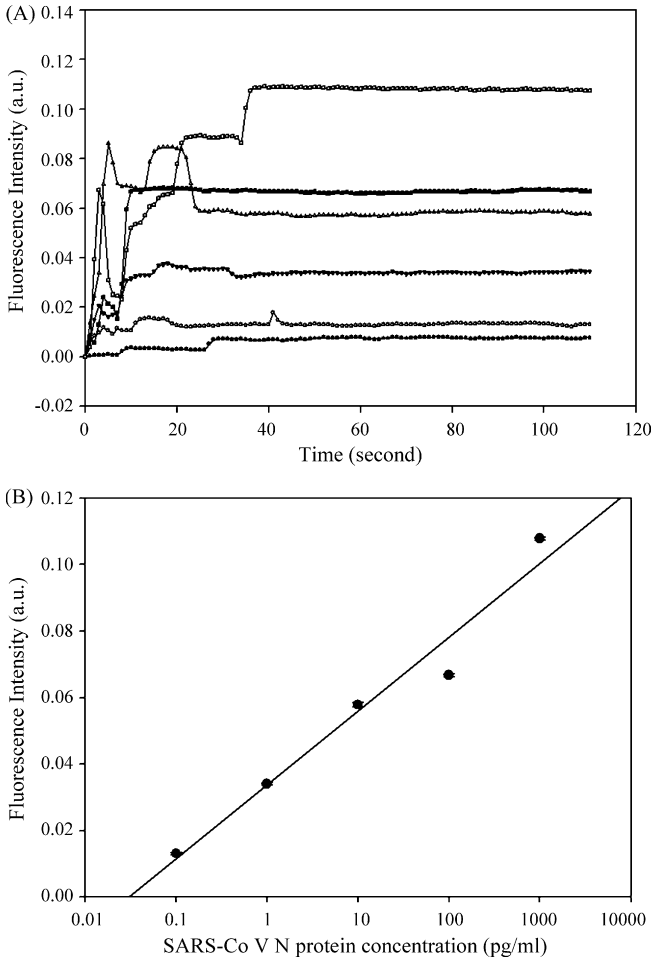

Fig. 3. Detection of different concentrations of GST-N protein in 10-fold diluted human serum with LSPCF fiber-optic biosensor. (A) The binding processes of fluorescence probe interaction with different concentrations of GST-N protein in diluted serum [●: 0 pg/mL; ○: 0.1 pg/mL; ▼: 1 pg/mL; ▽: 10 pg/mL; ■: 100 pg/mL; □: 1000 pg/mL]. The uncertainty of the measurement is smaller than the size of data points in this figure. (B) The linear relationship [$y = 0.0096\,\mathrm{Ln}(x) + 0.0337$; $R^2 = 0.9624$] of GST-N protein concentration in diluted serum versus fluorescent signal. The error bar is smaller than the size of data points and equivalent to one standard derivation in this experiment.

in Fig. 2B clearly. The correlation coefficient (R^2) is 0.9469 and the error bar is equal to one standard deviation.

In order to demonstrate that LSPCF fiber-optic biosensor can be applied to clinical specimens, we prepared GST-N proteins in 10-fold diluted serum. Fig. 3A shows the temporal fluorescence intensity of the biomolecular interaction between the LSPCF probes and GST-N proteins at different concentrations in diluted serum. Again, a clear linear relationship between the fluorescence signal and the different concentrations of GST-N protein in diluted serum over the range from 0.1 pg/mL to 1 ng/mL is presented in Fig. 3B. The correlation coefficient (R^2) is 0.9624 in this experiment and the error bar is a standard deviation. From the data, the detection limit for GST-N protein in real serum samples should be around 1 pg/mL because the LSPCF technique can distinguish between the signal from a sample containing 0.1 pg/mL of target protein and the noise generated by the other serum proteins present in 10-fold diluted serum.

4. Discussions

In this study, we generated two monoclonal antibodies against SARS-CoV N protein tagged with GST. Using conventional antigen capture ELISA, GST-N protein was detectable at a concentration as low as 15 ng/mL in PBS or 1 ng/mL in diluted serum. In order to enhance the detection sensitivity, a highly sensitive LSPCF fiber-optic biosensor was used. The lowest detectable concentration in PBS was verified experimentally to be 0.1 pg/mL. Furthermore, the detection limit in 10-fold diluted human serum was 0.1 pg/mL, which is equivalent to 1 pg/mL in undiluted serum. In other studies using conventional ELISA, the detection limits for recombinant SARS-CoV N protein were stated to be 37.5 (He et al., 2005), 50 (Che et al., 2004), 200 (Lau et al., 2004), and 1000 pg/mL (Shang et al., 2005). Only the CLEIA based system which detects protein levels as low as 1.56 pg/mL of recombinant SARS-CoV N protein (Fujimoto et al., 2008), is comparable to our method. However, CLEIA requires tedious washing steps and is relatively prone to methodological variations. Although our conventional ELISA system is not as sensitive as those methods presented in other reports, our developed LSPCF platform improves sensitivity up to at least 10^4-fold using the same monoclonal antibodies. Therefore, in terms of detection limit and cost effectiveness, the LSPCF fiber-optic biosensor becomes one of the best methods for SARS-CoV N protein detection in human serum. Furthermore, the LSPCF system has a great potential to become a high throughput chip-based assay in the measurement of serum protein levels qualitatively and quantitatively.

The ultra low detection limit of LSPCF fiber-optic biosensors is based on several properties. Firstly, the LSPs excite and enhance fluorescence with high efficiency near the GNP surface. Secondly, the fluorescence is amplified because more than 40 fluorophores are presented on each fluorescence probe and excited simultaneously. Thirdly, on the fluorescence probe, the protein A which is immobilized on the GNP surface, acts not only as a linker by connecting to the secondary antibody labeled fluorophore but also as a spacer that avoids metal-induced quenching effects effectively (Hsieh et al., 2007). Fourthly, the fluorescence signal is detected at the distal end of the optical fiber in a conventional setup. In such situations, the coaxial propagation of the pumping laser beam induces a strong background signal, which results in a lower detection limit apparently. In contrast, the LSPCF fiber-optic biosensor detects the fluorescence signals close to the reaction region (Hsieh et al., 2007; Chang et al., 2009). It results in a significant increase in the fluorescence collection efficiency compared with the conventional setup (Chang et al., 1996). Finally, the sandwich immunoassay configuration in the LSPCF biosensor exhibits better specificity than other types of immunoassays such as direct labeling and single-capture (Kingsmore, 2006). The LSPCF fiber-optic biosensor has many useful features such as ease of operation and disposability. In addition, based on the ultra high detection sensitivity and quantitative ability, this biosensor can be used for the early diagnosis of diseases in clinics.

5. Conclusions

In this study, the LSPCF fiber-optic biosensor demonstrated a detection sensitivity of 1 pg/mL for GST-N protein in human serum. This level is very suitable for application to the clinical diagnosis at the early stage of SARS patients. Importantly, a linear response between the fluorescence signal and the concentration of GST-N protein was obtained for a range from 0.1 pg/mL to 1 ng/mL. In comparison with conventional antigen capture ELISA, the detection limit of the LSPCF fiber-optic biosensor for GST-N protein has been shown to be increased by 10^4-fold using the same monoclonal antibodies. Finally, the linear relationship between the concentration of GST-N protein in diluted serum and fluorescence signal indicates that the LSPCF biosensor, when used for the clinical diagnosis of SARS-CoV infection, should be able to work well at a very early stage of infection among SARS patients.

Acknowledgements

This research was supported by National Science Council of Taiwan through the Research Grants NSC 97-2627-B-008-001 and NSC 96-2221-E-010-002-MY2 to C. Chou and NSC 97-2320-B-010-011-MY3 to J.C. Huang and NSC 97-2321-B-010-003 to Y.M.A. Chen. *Ling Yao* for participation in the antibody purification and Prof. Ralph Kirby for manuscript revision are also appreciated. This research was supported in part by "Aim for the Top University Plan" of National Yang-Ming University.

Appendix A. Supplementary data

Supplementary data associated with this article can be found, in the online version, at doi:10.1016/j.bios.2009.07.012.

References

Abad-Valle, P., Fernandez-Abedul, M.T., Costa-Garcia, A., 2005. Biosens. Bioelectron. 20, 2251–2260.
Chan, P.K.S., Liu, E.Y.M., Leung, D.T.M., et al., 2005. J. Med. Virol. 75, 181–184.
Chang, Y.-H., Chang, T.-C., Kao, E.-F., et al., 1996. Biosci. Biotechnol. Biochem. 60, 1571–1574.
Chang, Y.-F., Chen, R.-C., Lee, Y.-J., et al., 2009. Biosens. Bioelectron. 24, 1610–1614.
Che, X.Y., Qiu, L.W., Pan, Y.X., et al., 2004. J. Clin. Microbiol. 42, 2629–2635.
Chen, S., Lu, D., Zhang, M., et al., 2005. Eur. J. Clin. Microbiol. Infect. Dis. 24, 549–553.
Cui, R.J., Huang, H.P., Yin, Z.Z., et al., 2008. Biosens. Bioelectron. 23, 1666–1673.
Drosten, C., Doerr, H.W., Lim, W., et al., 2004. Emerg. Infect. Dis. 10, 2200–2203.
Fouchier, R.A.M., Kuiken, T., Schutten, M., et al., 2003. Nature 423, 240–1240.
Fujimoto, K., Chan, K.H., Takeda, K., et al., 2008. J. Clin. Microbiol. 46, 302–310.
Haynes, L.M., Miao, C., Harcourt, J.L., et al., 2007. Clin. Vaccine Immunol. 14, 331–333.
He, Q.G., Du, Q.Y., Lau, S.L., et al., 2005. J. Virol. Methods 127, 46–53.
Hong, T.C., Mai, Q.L., Cuong, D.V., et al., 2004. J. Clin. Microbiol. 42, 1956–1961.
Hourfar, M.K., Roth, W.K., Seifried, E., et al., 2004. J. Clin. Microbiol. 42, 2094–2100.
Hsieh, B.-Y., Chang, Y.-F., Ng, M.-Y., et al., 2007. Anal. Chem. 79, 3487–3493.
Jiang, S.S., Chen, T.C., Yang, J.Y., et al., 2004. Clin. Infect. Dis. 38, 293–296.
Jung, L.S., Campbell, C.T., Chinowsky, T.M., et al., 1998. Langmuir 14, 5636–5648.
Kingsmore, S.F., 2006. Nat. Rev. Drug Discov. 5, 310–320.
Lau, S.K.P., Woo, P.C.Y., Wong, B.H.L., et al., 2004. J. Clin. Microbiol. 42, 2884–2889.
Li, Y.H., Li, J., Liu, X.E., et al., 2005. J. Virol. Methods 130, 45–50.
Liu, I.J., Chen, P.J., Yeh, S.H., et al., 2005. J. Clin. Microbiol. 43, 2444–2448.
Louie, L., Simor, A.E., Chong, S., et al., 2006. J. Clin. Microbiol. 44, 4193–4196.
Manopo, I., Lu, L.Q., He, Q.G., et al., 2005. J. Immunol. Methods 296, 37–44.
Manso, J., Mena, M.L., Yanez-Sedeno, P., et al., 2008. Anal. Biochem. 375, 345–353.
Marra, M.A., Jones, S.J., Astell, C.R., et al., 2003. Science 300, 1399–1404.
McFarland, A.D., Van Duyne, R.P., 2003. Nano Lett. 3, 1057–1062.
Mock, J.J., Smith, D.R., Schultz, S., 2003. Nano Lett. 3, 485–491.
Peiris, J.S.M., Lai, S.T., Poon, L.L.M., et al., 2003a. Lancet 361, 1319–1325.
Peiris, J.S.M., Chu, C.M., Cheng, V.C.C., et al., 2003b. Lancet 361, 1767–1772.
Petrich, A., Mahony, J., Chong, S., et al., 2006. J. Clin. Microbiol. 44, 2681–2688.

Poon, L.L.M., Leung, C.S.W., Tashiro, M., et al., 2004. Clin. Chem. 50, 1050–1052.
Poon, L.L.M., Wong, B.W.Y., Chan, K.H., et al., 2005. J. Clin. Microbiol 43, 3457–3459.
Qiu, M.F., Wang, J., Wang, H.X., et al., 2005. Clin. Diagn. Lab. Immunol. 12, 474–476.
Rota, P.A., Oberste, M.S., Monroe, S.S., et al., 2003. Science 300, 1394–1399.
Shang, B., Wang, X.-Y., Yuan, J.-W., et al., 2005. Biochem. Biophys. Res. Commun. 336, 110–117.
Shi, Y., Yi, Y., Li, P., et al., 2004. J. Clin. Microbiol. 41, 5781–5782.
Sonnichsen, C., Franzl, T., Wilk, T., et al., 2002. Phys. Rev. Lett. 88, 077402.
Wang, W.K., Chen, S.Y., Liu, I.J., et al., 2004. Emerg. Infect. Dis. 10, 1213–1219.
Wang, B., Potter, S.J., Lin, Y.G., et al., 2005. J. Clin. Microbiol. 43, 2339–2344.
Yam, W.C., Chan, K.H., Poon, L.L.M., et al., 2003. J. Clin. Microbiol. 41, 4521–4524.
Yu, F., Persson, B., Lofas, S., et al., 2004. Anal. Chem. 76, 6765–6770.
Zhao, J.C., Wang, W., Wang, G.F., et al., 2005. J. Clin. Virol. 33, 12–18.